Comparative Medicine
Copyright 2013
by the American Association for Laboratory Animal Science

Vol 63, No 1
February 2013
Pages 13–21

Original Research

Comparison of Vascular Leak Syndrome in Mice Treated with IL21 or IL2

Pallavur V Sivakumar, Richard Garcia, Kimberly S Waggie,* Monica Anderson-Haley, Andrew Nelson, and Steven D Hughes

Interleukin 21 (IL21) is a T-cell–derived 4-helix–bundle cytokine that has sequence homology to the IL2 family. Recombinant human interleukin 2 (rIL2) is approved for the treatment of metastatic melanoma and renal cell carcinoma. However, toxicity of rIL2, including induction of vascular leak syndrome (VLS), has limited use of this cytokine to a small proportion of eligible patients. Both rIL2 and murine IL21 (mIL21) have potent antitumor efficacy in murine models. The purpose of the current study was to compare the ability of mIL21 and rIL2 to induce vascular leakage in a mouse model. Pulmonary and hepatic uptake of Evans blue dye, serum cytokine levels, spleen cell immunophenotype, and histologic changes in lung and liver were evaluated to detect VLS. High-dose (200 µg) rIL2 treatment induced vascular leakage in mice, evidenced by inflammatory cell infiltration and fluid extravasation into the lung and liver and increased levels of TNFα, IFNγ, IL5, MCP1, and IL6 in serum. In contrast, an equivalent dose of mIL21 resulted in minimal vascular leakage with no evidence of cytopenia or cytokine production. These results support the use of IL21 as a cancer immunotherapeutic agent, potentially providing an antitumor response without induction of VLS.

Abbreviations: mIL21, murine IL21; NK, natural killer; rIL2, recombinant human interleukin 2; VLS, vascular leak syndrome.

Immunotherapy with recombinant human interleukin 2 (rIL2) is an approved treatment for metastatic melanoma and renal cell carcinoma.[22,23,29,31] However, use of rIL2 as a therapeutic agent in the clinic has been limited by its dose-dependent toxicity, characterized by acute respiratory failure and hemodynamic instability. This combination of symptoms is associated with increased microvascular permeability andhas been termed vascular leak syndrome (VLS).[5,37] rIL2-induced VLS is characterized by transendothelial migration of inflammatory cells, including neutrophils and lymphocytes, into the lung and other tissues resulting in tissue damage. Acute organ injury is mediated by activated neutrophils which cause endothelial damage through production of reactive oxygen metabolites and other proinflammatory factors. In addition, neutrophils can cause microcirculatory occlusion, leading to decreased tissue perfusion. Chronic organ injury is mediated by infiltrating mononuclear cells, including lymphocytes and natural killer (NK) cells.[21] Increased production of cytokines, such as TNFα, has been implicated in lymphocyte infiltration into the lung and subsequent lung injury.[13] VLS has limited the use of rIL2 to a restricted population of patients based on age and other narrow eligibility criteria.[33] Therefore, there is a need for cancer immunotherapeutic agents with improved safety profiles compared with that of rIL2.

Interleukin 21 (IL21) is a 4-helix–bundle cytokine that has sequence homology to IL2.[4,20,26] IL21 mediates its effects by binding to a unique IL21 receptor subunit, which forms a heterodimer with the common γ-chain (γc) shared with other members of the IL2 cytokine family.[4] The IL21 receptor is expressed primarily on NK cells, $CD4^+$ and $CD8^+$ T cells, B cells, and dendritic cells.[35] IL21 enhances the cytolytic activity of NK cells and $CD8^+$ T cells and has efficacy in multiple mouse tumor models.[10,35] In addition, IL21 costimulates differentiation of B cells into antibody-producing plasma cells.[15,25] IL21 is therefore a prime candidate for a cancer immunotherapeutic and has been evaluated in clinical trials for treatment of metastatic melanoma and renal cell carcinoma.[9,11,12]

In mice, VLS can be induced with administration of repeated high doses of rIL2, and the extent of change in capillary permeability can be measured by the accumulation of Evans blue dye in the lung and other tissues.[30] Other parameters that have been shown to be characteristic of VLS in mice include increased numbers of activated T cells, NK cells, and monocytes in the liver, lung, and kidney; upregulated expression of adhesion molecules (that is, LFA1, VLA4, and ICAM1) on lymphocytes and monocytes; and increased serum levels of TNFα and IFNγ.[2] In mice, depletion of cells with surface phenotypes characteristic of NK–T or NK cells ameliorates organ damage.[3,17] Increased numbers of NK cells and monocytes in the lung and liver therefore are considered to be biomarkers for rIL2-mediated cellular effects of VLS.

The aim of the current study was to compare the ability of rIL2 and murine IL21 (mIL21) to induce VLS in mice. Mice were injected with equivalent doses of either rIL2 or mIL21 under conditions in which rIL2 has been shown to induce vascular leakage. Parameters indicative of VLS (Evans blue uptake, serum cytokine analysis, spleen cell immunophenotype) were measured, and tissues were evaluated microscopically for evidence of inflammatory cell infiltrates. In contrast to rIL2, mIL21 did not induce VLS in mice and did not cause the cytokine induction or multiorgan inflammation characteristic of rIL2-induced toxicity.

Received: 17 May 2012. Revision requested: 21 Jul 2012. Accepted: 21 Aug 2012.
ZymoGenetics, a Bristol-Myers Squibb Company, Seattle, Washington.
**Corresponding author. Email: kim.waggie@bms.com*

Materials and Methods

Mice. Female C57BL/6N mice (*Mus musculus*; Charles River Laboratories, Wilmington, MA) between 8 and 12 wk of age (weight, 18 to 20 g) were used for all studies. The mice were free of common bacterial pathogens, including *Helicobacter* spp., and ecto- and endoparasites and were negative for: Sendai virus, pneumonia virus of mice, mouse hepatitis virus, minute virus of mice, Theiler disease virus, reovirus 3, lymphocytic choriomeningitis virus, ectromelia virus, epizootic diarrhea of infant mice virus, murine parvovirus, K virus, polyoma virus, mouse adenovirus, mouse cytomegalovirus, and hantavirus. Mice were kept on a 12:12-h light:dark cycle, housed on corn cob bedding (Bed-o'Cobs, The Andersons, Maumee, OH) in ventilated microisolation caging (Lab Products, Seaford, DE), and given deionized water and autoclaved rodent chow (Purina Rodent Chow 5053, Purina Mills, St Louis, MO) ad libitum. All procedures were approved by the ZymoGenetics IACUC and followed the guidelines set forth in the *Guide for the Care and Use of Laboratory Animals*.[19]

Reagents. Recombinant mIL21 (ZymoGenetics, Seattle, WA) was stored at −80 °C as a frozen solution in PBS (pH 6.0). Full-length mIL21 was expressed by using a baculovirus system.[6] Recombinant IL2 (Aldesleukin Proleukin, Chiron, Emeryville, CA) was reconstituted and diluted according to the manufacturer's recommendations. Vehicle used in these studies was PBS 1×, pH 7.2 (Invitrogen, Carlsbad, CA).

Vascular leak model. Three studies were performed, 2 of which involved 5 groups of 10 mice each. The mice received intraperitoneal injections of PBS, rIL2 (33 or 100 µg), or mIL21 (33 or 100 µg) twice daily for a total of 7 doses. Doses and regimens were chosen in light of data regarding IL2-induced VLS.[16,32] Murine IL21 was selected for comparison to rIL2 because recombinant human IL21 lacks activity on several key lineages of mouse cells (data not shown). Doses were calculated on a weight-to-weight basis so that rIL2 and mIL21 were dosed in mass-equivalent (and approximately equimolar) amounts. The doses of mIL21 were comparable to or greater than those reported to be efficacious in murine xenogenic tumor models.[14,24,34] Body weights were monitored daily. Evans blue dye was administered intravenously via the tail vein (0.2 mL, 1% solution) 2 h after the final cytokine injection on day 4. Exactly 2 h after Evans blue injection, mice were anesthetized with isoflurane, and blood was withdrawn for cytokine and hematology analysis. CBCs were performed by using an automated blood analyzer (Cell-Dyn 3500, Abbot Laboratories, Santa Clara, CA). Mice then were perfused transcardially with 10 mL heparinized saline (25 U heparin per milliliter saline; flow rate, 5 mL/min). After perfusion, the spleen and liver were removed and weighed. Vascular leakage was measured in lung and liver as previously described.[30] Briefly, after transcardial perfusion, both lung and liver were excised, rinsed with PBS, blotted on gauze, placed into 10 mL formamide, and incubated at 37 °C for 24 h. After incubation, the absorbance of the supernatant at 650 nm was measured and compared against a standard curve of Evans blue dissolved in formamide. The mice in the second of these studies had also been implanted with a transponder to monitor body temperature (see below).

In the third study involving 7 groups of 4 mice each, body temperature was monitored daily by using a programmable temperature transponder (Biomedic Data System, Seaford, DE). Three days prior to study initiation, mice were anesthetized with isoflurane, and the transponder was implanted aseptically into the abdominal cavity and anchored to the abdominal wall. Antibiotics (2.5 mg/kg IM; Baytril, Bayer Animal Health, Shawnee Mission, KS) were administered immediately before and for 2 d after surgery, and buprenorphine (2.5 mg/kg SC) was provided immediately after surgery and as needed thereafter. The mice received intraperitoneal injections of PBS, rIL2 (33, 100, or 200 µg), or mIL21 (33, 100, or 200 µg) twice daily for a total of 7 doses. Two hours after the final cytokine injection, mice were anesthetized with isoflurane, and blood was withdrawn for cytokine and hematology analysis. Body, splenic, and hepatic weights were obtained at necropsy, spleens were harvested for immunophenotyping, and tissues collected into 10% neutral buffered formalin for routine histopathology.

Serum cytokine measurements. Mice were anesthetized by using isoflurane, and blood was collected via retroorbital puncture. Serum was separated by using standard serum separator tubes. Multiple cytokines in the serum from each mouse were measured by using cytokine bead-array kits. The mouse Th1/Th2 Cytokine and mouse Inflammation Cytokine Bead Array Kits (Becton Dickenson, San Diego, CA) were used according to the manufacturer's instructions.

Immunophenotyping of splenic cells. Spleens were isolated from 4 euthanized mice per group and placed in complete RPMI media containing 5% FBS. Cell suspensions were derived by pressing spleens gently between 2 frosted slides, suspending the material in RPMI containing 5% FBS, and centrifuging for 5 min at 300 × *g*. RBC were lysed by incubating cell suspensions in ACK lysis buffer (0.15 M NH_4Cl, 1 mM $KHCO_3$, 0.1 mM EDTA) for 4 min, followed by neutralization in RPMI containing 10% FBS. The expression of cell surface markers was analyzed by standard 3-color flow cytometry; all antibodies were obtained from Pharmingen (San Diego, CA). FITC-conjugated CD11a (LFA1), CD49d (VLA4, α chain), and Gr1; phycoerythrin-conjugated CD4, NK1.1, and CD11b; and CyC-conjugated CD8, CD3, and B220 were used to stain cells. Nonspecific binding was blocked by incubating cells in blocking buffer (PBS, 10% FBS, 20 µg/mL antiCD16/CD32 [clone 2.4G2, Becton Dickenson]). After blocking, cells were incubated with primary antibodies for 20 min at room temperature; unless specified otherwise, antibody staining occurred in a 100-µL volume, with a final antibody concentration of 10 µg/mL. Cells were washed once in PBS and resuspended in PBS before measurement of fluorescence (FACScan or FACSCalibur, Becton Dickinson). Data were analyzed by using Cellquest software (Becton Dickinson). Cell population percentages were converted to cell numbers by using the spleen cell count obtained for the sample.

Histopathology. For histopathology, parallel cohorts of mice were injected with the indicated cytokines at the specified doses and times, but the mice did not receive Evans blue dye before termination of the experiment. Liver, lung, brain, kidney, pancreas, and intestine from 4 mice per group were collected into 10% neutral buffered formalin, routinely processed into paraffin blocks, sectioned at 5 µm by using a rotary microtome (model 2155, Leica Microsystems, Nusslock, Germany), and stained with hematoxylin and eosin in an automated slide stainer (Jung AutoStainer XL, Leica Microsystems). The tissues were evaluated in blinded fashion by a board-certified veterinary pathologist. Changes were noted, and disease severity was scored as follows: 1, minimal; 2, mild; 3, moderate; and 4, severe.

Statistical analysis. Data from each study underwent ANOVA with posthoc analysis of pairwise differences by using Fisher

Protected Least Significant Difference tests (StatView version 5.0.1, SAS Institute, Cary, NC). Statistical significance was defined as a P value of less than 0.05.

Results

rIL2 induces enhanced vascular permeability in lung and liver. All mice survived treatment with 33, 100, or 200 µg rIL2 or mIL21. No obvious physical differences were observed between mice given PBS or mIL21 at any of the doses tested. However, mice treated with rIL2 demonstrated clinical signs, which increased in severity in a dose- and time-dependent manner. On the final day of the study (day 4), rIL2-treated mice displayed decreased activity, decreased food consumption, and piloerection. Body weight decreased significantly ($P < 0.05$) between days 1 and 4 in mice treated with either 100 µg or 200 µg rIL2 but not in those treated with PBS or mIL21 (Figure 1 A). Body temperature similarly decreased ($P < 0.05$) over the course of the study in mice treated with 100 or 200 µg rIL2 compared with their own baseline weight and relative to that of mice treated with PBS or any dose of mIL21 (Figure 1 B).

Vascular permeability as measured by Evans blue extravasation into the lung was increased markedly at both dose levels of rIL2 (100 and 200 µg) compared with PBS (Figure 1 C). The lungs of mice treated with 100 or 200 µg rIL2 showed a 3- to 4-fold increase in Evans blue dye content, compared with those of PBS-treated controls. Mice treated with 200 µg but not 100 µg mIL21 demonstrated increased Evans blue dye content relative to that of PBS-treated controls. However, mIL21-associated Evans blue extravasation was approximately half that after treatment with mIL21, considering the mass-equivalent doses used.

We also evaluated the liver vascular leakage. Despite the lower sensitivity of this tissue to changes in capillary permeability, we noted increased levels of Evans blue in the livers of mice treated with either 100 or 200 µg rIL2 (Figure 1 D). In contrast, the

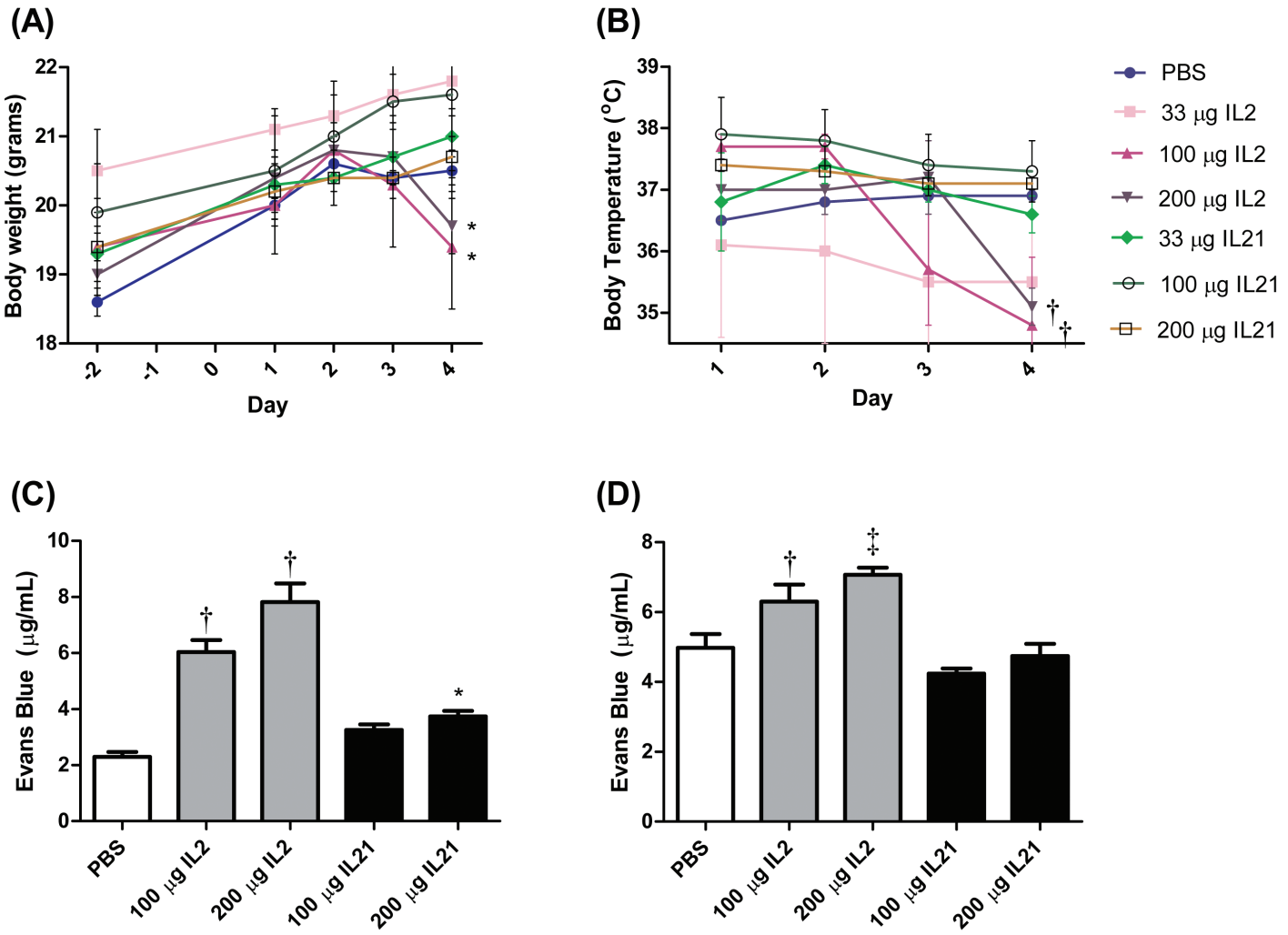

Figure 1. Body weight, body temperature, and vascular leakage in mice (n = 4 to 6 mice per group) injected with 33, 100, or 200 µg rIL2 (IL2) or mIL21 (IL21) twice daily for a total of 7 doses. Body weights were recorded at baseline (day –2), and (A) weights and (B) body temperatures were monitored during the experiment. At 2 h after the final dose, mice were injected intravenously with Evans blue dye, and (C) lungs and (D) livers were isolated and analyzed for vascular leak as measured by Evans blue extravasation (mean values ± SEM). White box, PBS treatment group; gray boxes, rIL2 treatment groups; black boxes, mIL21 treatment groups. Value significantly (*, $P < 0.05$; †, $P < 0.01$; ‡, $P < 0.001$) different from that for day 1 baseline (weight and temperature) or PBS control (Evans blue). Data are shown are representative of 1 of 3 experiments performed.

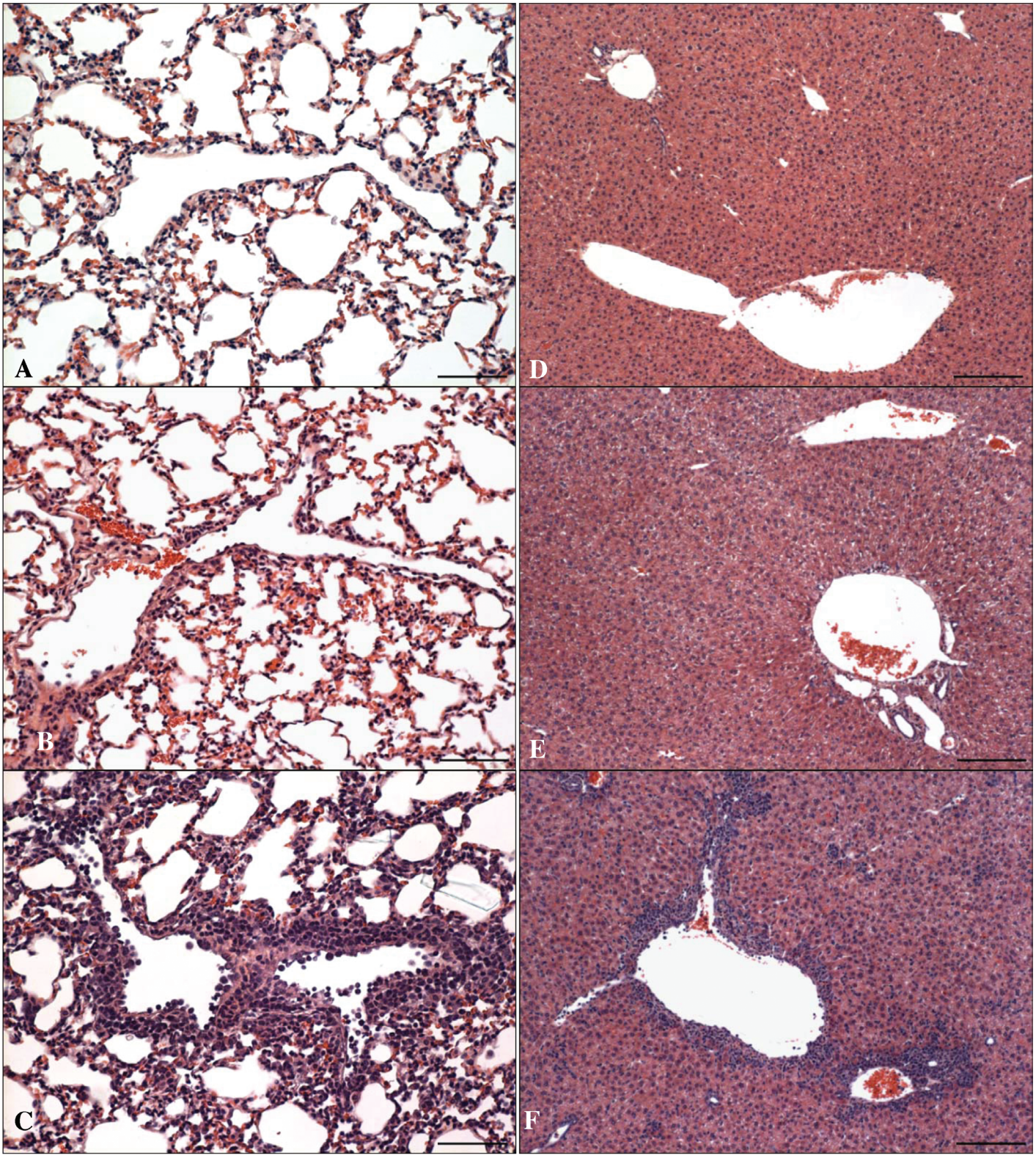

Figure 2. Histopathology of mice (n = 4 mice per group) injected with 33, 100, or 200 µg rIL2 (IL2) or mIL21 (IL21) twice daily for a total of 7 doses. At the termination of the experiment (day 4), lung and liver were collected into neutral buffered formalin for processing with hematoxylin and eosin. Representative images of (A through C) lung and (D through F) liver sections from mice treated with either (A and D) PBS (control), (B and E) 200 µg mIL21, or (C and F) 200 µg rIL2 are shown. Treatment with rIL2 increased numbers of mononuclear inflammatory cells in and around the vasculature, as compared with mIL21 and PBS. Scale bar, 62 µm (A through C) or 123 µm (D through F).

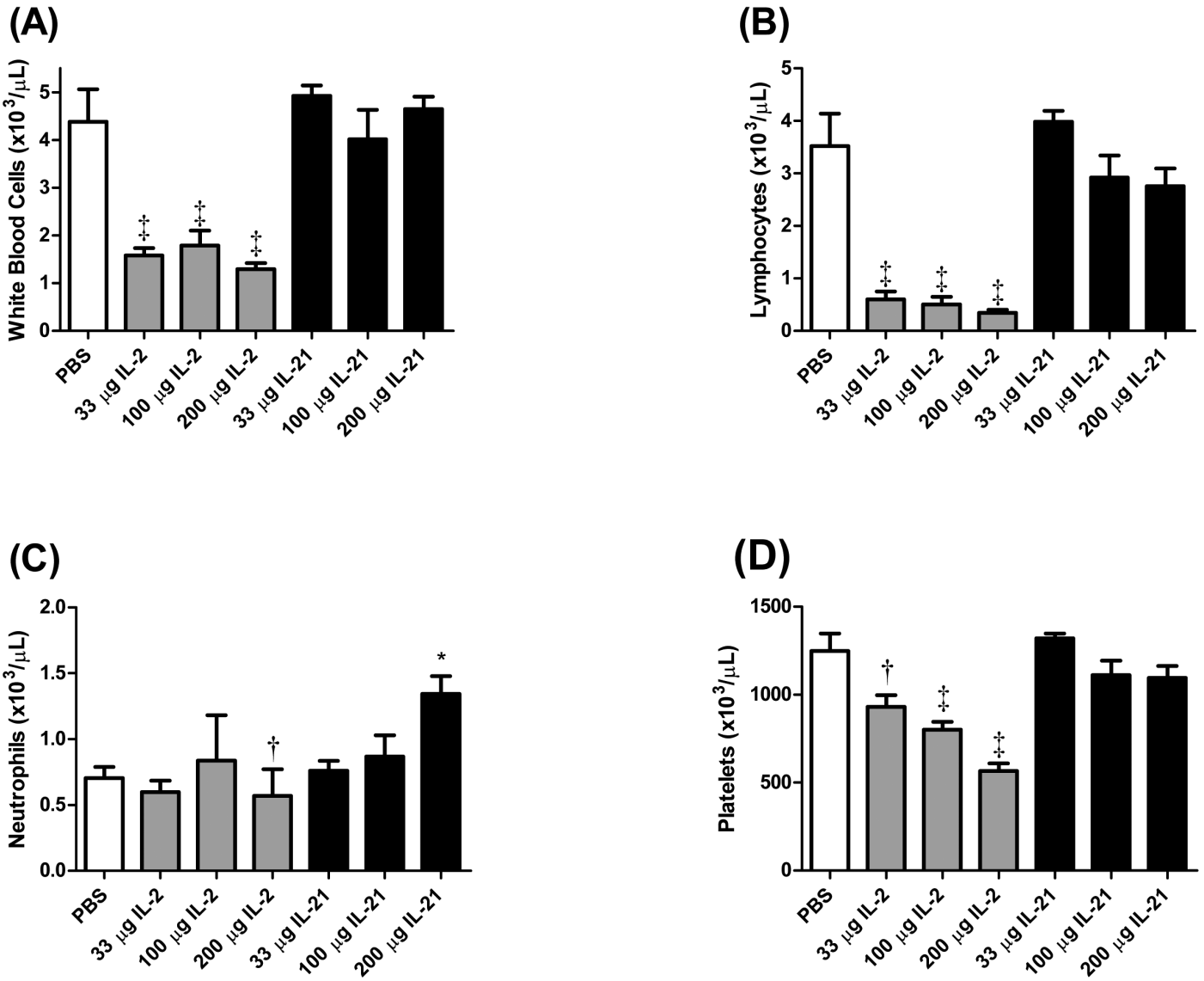

Figure 3. Hematology of mice (n = 4 to 6 mice per group) injected with 33, 100, or 200 µg rIL2 (IL2) or mIL21 (IL21) twice daily for a total of 7 doses. At the termination of the experiment (day 4), blood was collected and analyzed for (A) WBC, (B) lymphocyte, (C) neutrophil, and (D) platelet counts (mean ± SEM). White box, PBS treatment group; gray boxes, rIL2 treatment groups; black boxes, mIL21 treatment groups. Value significantly (*, $P < 0.05$; †, $P < 0.01$; ‡, $P < 0.001$) different from that for the PBS control.

Evans blue dye contents of livers from mice treated with 100 or 200 µg mIL21 did not differ from that of control mice. Hepatic weights at necropsy were normalized to body weights; we then compared the normalized hepatic weights of the PBS, rIL2, and mIL21 groups to determine whether treatment-related changes were present. Relative hepatic weights were increased at all dose levels of rIL2 and at the 200-µg dose of mIL21, compared with those after PBS (data not shown).

Multiorgan inflammation is greater in rIL2-treated mice. Microscopic examination of livers and lungs revealed that inflammatory changes were more common and more severe in rIL2- than mIL21-treated mice (Figure 2). In the lung, vascular inflammation was the primary finding in the rIL2- and mIL21-treated mice; this change was not present in the control group. Vasculitis in the rIL2 group was characterized by the presence of numerous mononuclear cells within the vascular lumen and wall and around the vessel. This infiltrate involved the majority of the large- diameter vessels in the lung. In contrast, inflammation in the mIL21-treated groups involved few vessels, was present in only a few foci per vessel cross-section, and was characterized by occasional intravascular mononuclear cells, swollen endothelial cells, and infrequent perivascular mononuclear cells. In addition, vasculitis was present in the livers of all of the rIL2-treated mice (Figure 2 B) and was accompanied by multifocal infiltrates of inflammatory cells scattered throughout the parenchyma. Low numbers of perivascular inflammatory cells were observed in the liver of only one of the mIL21-treated mice at each dose level. Inflammatory cell infiltrates were not present in the livers of control mice. In addition, significantly ($P < 0.05$) increased numbers of mononuclear infiltrates were present in the brain, kidney, pancreas, and intestine of rIL2- but not mIL21-treated mice.

Hematologic alterations are present after rIL2 treatment. Significant ($P < 0.05$) decreases in WBC counts and circulating lymphocytes were observed in mice treated with all doses of rIL2 tested (Figure 3 A and B). Lymphocyte and WBC counts in mice treated with mIL21 were not significantly different from those of PBS-treated mice. Neutrophil counts were decreased ($P < 0.01$) slightly in mice treated with 200 µg rIL2. In contrast, neutrophil counts were increased ($P < 0.05$) after the 200-µg dose of mIL21, as compared with either PBS or the equivalent dose of rIL2 (Figure 1 C). A dose-dependent decrease ($P < 0.05$) in circulating platelet count occurred in mice treated with rIL2, whereas platelet counts in mIL21-treated mice did not differ from those of the PBS control group (Figure 1 D).

Splenic weight, cellularity, and phenotype change after rIL2 or mIL21 administration. rIL2- and mIL21-treated mice had significantly ($P < 0.05$) increased splenic weights compared with those of the PBS-treated control groups (Table 1). Splenic weights in mIL21-treated mice were significantly ($P < 0.05$) less than those for the corresponding rIL2-treated groups. The increases in splenic weights in both groups were dose-dependent. Furthermore, high doses of rIL2 significantly increased splenic cellularity over that of control groups (Table 1). Splenic cellularity did not differ between the rIL21- and PBS- treated groups.

Flow cytometry of spleen cells revealed that rIL2-treated mice had dose-dependent increases in the numbers and relative percentages of NK–T cells ($NK1.1^+CD3^+$), NK cells ($NK1.1^+CD3^-$), macrophages ($CD11b^+$), granulocytes ($Gr1^+$), and $LFA1^+$ cells (Table 2). rIL21-treated mice had no increase in NK–T, NK, or $LFA1^+$ cells at any dose. However, the percentages and numbers of macrophages ($CD11b^+$; 100 µg and 200 µg doses) and granulocytes ($Gr1^+$; 200 µg dose) were increased ($P < 0.05$) in the mIL21-treated group compared with the control group. The increases in macrophage and granulocyte percentages and numbers observed in the mice treated with high-dose mIL21 were comparable to those seen in rIL2-treated mice.

rIL2—but not mIL21—administration induces an inflammatory cytokine response in mice. Treatment of mice with various doses of rIL2 dramatically increased the levels of inflammatory cytokines in the serum, namely TNFα, IFNγ, IL5, MCP1, and IL6 (Figure 4). Mice treated with mIL21 did not show any significant ($P < 0.05$) changes in cytokine levels. Several other cytokines (IL4, IL10, IL2) showed no upregulation after the administration of either cytokine (data not shown).

Table 1. Spleen weight and cellularity (mean ± SEM)

Treatment	Spleen weight: body weight	Spleen cellularity ($\times 10^6$ cells)
PBS	0.0030 (0.0004)	47.97 (8.214)
33 µg IL2	0.0082 (0.0004)[c]	57.09 (5.887)
100 µg IL2	0.0106 (0.0005)[c]	100.4 (10.81)[c]
200 µg IL2	0.0133 (0.0016)[c]	101.8 (2.13)[c]
33 µg IL21	0.0044 (0.0001)[a]	58.84 (6.762)
100 µg IL21	0.0055 (0.0004)[b]	47.69 (3.919)
200 µg IL21	0.0061 (0.0007)[b]	53.76 (11.25)

[a]Value significantly ($P < 0.05$) different from that of the PBS treatment (control) group.
[b]Value significantly ($P < 0.01$) different from that of the PBS treatment (control) group.
[c]Value significantly ($P < 0.001$) different from that of the PBS treatment (control) group.

Discussion

VLS is the primary dose-limiting side effect of rIL2 therapy in humans. The mechanisms underlying this toxicity are not entirely understood, but critical events and mediators have been identified.[5,21] Essentially, damage occurs within the postcapillary endothelium, with adhesion and extravasation of activated leukocytes. Products of these cells activate and damage endothelial cells, leading to increased inflammatory cell chemotaxis and vascular permeability. Because blocking TNFα ameliorates lymphocyte infiltration and lung injury associated with rIL2 toxicity in mice, the production of TNFα secondary to administration of exogenous rIL2 appears to be critical for the development of VLS.[13]

In the current mouse study, we noted marked vascular leakage in both the lung and liver after treatment with rIL2. Serum concentrations of the cytokines TNFα, IFNγ, IL5, MCP1, and IL6 increased as well, and body temperature, body weight, and numbers of circulating lymphocytes and platelets all decreased after rIL2 treatment. These results are consistent with published reports on rIL2-induced VLS in mice.[27,30] In contrast, mIL21-treated mice showed only mildly increased vascular permeability only at the highest dose level. Although vascular permeability was elevated statistically significantly above PBS control levels, inflammatory changes in the lungs of mIL21-treated mice were much less severe than those observed with rIL2 treatment and were not associated with elevated serum cytokines or significant changes in hematologic parameters. In addition, body weight and temperature were unaffected in mIL21-treated mice. For the majority of parameters measured, the changes observed in mice treated with rIL2 were dose-dependent. In mIL21-treated mice, changes—when present—occurred only at the highest dose level and were much less severe than those in rIL2-treated mice.

Splenic weights were significantly increased in mice treated with either rIL2 or mIL21; this effect was greater in rIL2-treated mice. Increased splenic weight in rIL2-treated mice was associated with increased splenic cellularity; flow cytometric analysis showed increased percentages of all cell lineages tested, relative to those in control animals. Splenic cellularity in mIL21-treated mice was not significantly different from that in control animals. However, flow cytometry revealed a small but significant dose-dependent increase in the numbers of $CD11b^+$ cells in mIL21-treated mice. Further analysis revealed that most of these cells were of the $CD11b^+Gr1^-$ phenotype (macrophages, dendritic cells); fewer cells of the $CD11b^+Gr1^+$ phenotype (granulocytes) were present (data not shown). However, whether the effect seen in these experiments was due to a direct or indirect effect of mIL21 on myeloid cells remains unclear. Increases in specific cell types after IL21 treatment have previously been reported in the literature. For example, increases in granulocytes and monocytes after mIL21 treatment occurred in a mouse air-pouch model.[28] That study also demonstrated that human monocytes and monocyte-derived macrophages expressed the IL21 receptor complex and that the macrophages responded to IL21 by making CXCL8, a neutrophil chemoattractant. In addition, transient increases in circulating monocytes were noted in preclinical studies of rIL21 in cynomolgus monkeys and to a lesser extent in Phase I trials of rIL21 in patients with metastatic melanoma or renal cell carcinoma.[9,11,36,38]

Table 2. Spleen cell lineages

	NKT		NK		CD11b		B220		CD4		CD8		LFA1		Gr1	
Treatment	No.	%	No.	%	No.	%	No.	%	No.	%	No.	%	No.	%	No.	%
PBS	0.33	0.7	1.54	3.2	3.19	6.6	24.34	50.0	10.19	22.0	6.58	14.3	5.41	11.2	1.11	2.2
33 µg rIL2	2.34	4.3[b]	5.33	9.3[b]	7.04	12.6[b]	25.23	43.9	10.16	17.6	5.77	10.2	16.60	29.3[b]	2.82	5.0[a]
100 µg rIL2	3.08	3.2[b]	14.29[c]	13.9[b]	14.16[c]	14.6[b]	43.63	43.8*	15.57	15.6[a]	11.62	11.6[a]	35.11	34.8[b]	7.65	8.0[b]
200 µg rIL2	3.15[c]	3.1[b]	14.59	14.3[b]	12.08[c]	11.9[b]	43.53	42.8*	15.13	14.9[a]	17.64[c]	17.3[b]	44.83[c]	44.0[b]	4.76	4.7*
33 µg rIL21	0.37	0.6	1.77	3.0	4.67	7.8	31.50	53.6	10.47	17.9	6.32	11.0	5.05	8.4	1.05	1.8
100 µg rIL21	0.30	0.6	1.33	2.8	5.35	11.4[a]	23.16	48.3	8.55	17.8	5.40	11.3	6.35	13.4	1.54	3.2
200 µg rIL21	0.56	1.0	1.86	3.4	8.46	16.2[a]	23.85	45.1	9.20	17.2	6.39	12.2	8.43	15.7	3.20	6.4[b]

Each group contained 4 mice. Data are given as the mean number (×10⁶) or percentage of spleen cells.
[a]Value significantly ($P < 0.05$) different from that of the PBS treatment (control) group.
[b]Value significantly ($P < 0.01$) different from that of the PBS treatment (control) group.
[c]Value significantly ($P < 0.001$) different from that of the PBS treatment (control) group.

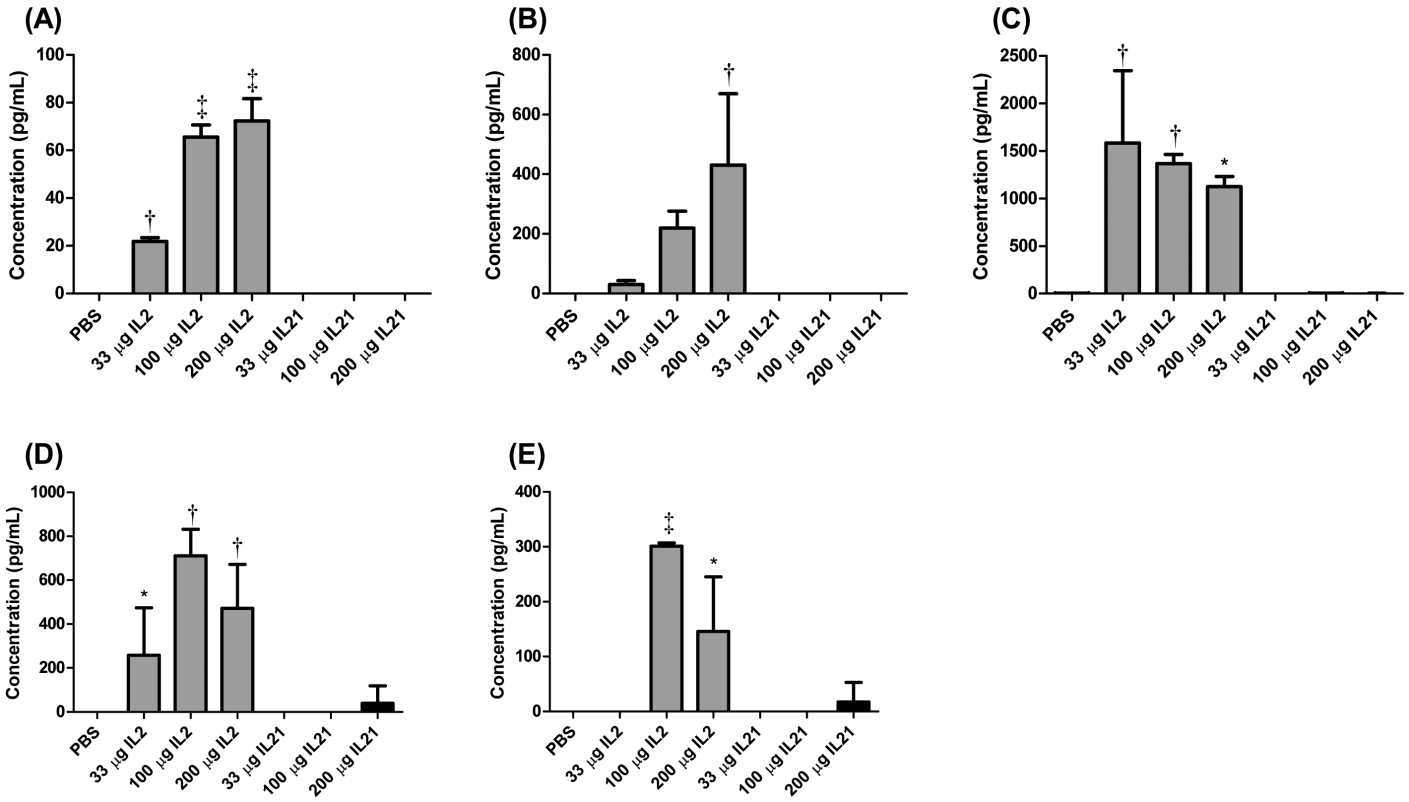

Figure 4. Serum levels (mean ± SEM) of the cytokines (A) TNFα, (B) IFNγ, (C) IL5, (D) MCP1, and (E) IL6 in mice (n = 4 to 6 mice per group) injected with 33, 100, or 200 µg of rIL2 (IL2) or mIL21 (IL21) twice daily for a total of 7 doses. At the termination of the experiment, serum was harvested from blood drawn from mice not injected with Evans blue dye, and cytokine concentrations were analyzed. White box, PBS treatment group; gray boxes, rIL2 treatment groups; black boxes, mIL21 treatment groups. Value significantly (*, $P < 0.05$; †, $P < 0.01$; ‡, $P < 0.001$) different from that for day 1 baseline (weight and temperature) or PBS control (Evans blue). Data are shown are representative of 1 of 3 experiments performed.

In contrast to the elevations in NK and NK–T cell numbers after rIL2 treatment, these populations did not change markedly after mIL21 treatment. However, both NK and NK–T cells have been shown to be activated with mIL21.[7,8] Furthermore, activation of NK cells has been demonstrated in rIL21-treated patients with melanoma.[9] The activation status of NK and NK–T cells was not evaluated in the current study.

Numbers of LFA1⁺ cells in our mice were increased after rIL2 treatment. LFA1 is thought to enable immune cells to bind activated endothelial cells and then transmigrate into tissue. Increased expression of LFA1 is considered a biomarker of rIL2-induced cellular activation during VLS.[2] LFA1⁺ cells did not increase in number after mIL21 treatment, consistent with the lack of VLS in mIL21-treated mice.

With regard to putative mechanisms of VLS, the most notable differences in the effects of mIL21 and rIL2 were the lack of cytokine elevation after mIL21 treatment and the different hematologic changes observed for the 2 treatment groups. TNFα

plays an important role in VLS development, and its levels were unchanged after treatment of mice with mIL21.[13] The reductions in lymphocyte and neutrophil counts in rIL2-treated mice were indicative of substantial leukocyte margination, another important event in the pathogenesis of VLS;[13] leukocyte margination did not occur in mIL21-treated mice. It is interesting to note that in preclinical studies in cynomolgus monkeys and in Phase I and II trials of rIL21 in renal cell carcinoma and melanoma, no signs of a 'cytokine storm' were noted.[9,11,36,38] Increases in TNFα and its soluble receptor, sTNF-RII, were seen in rIL21 clinical trials.[12] Although not compared directly in a single study, both rIL21 and rIL2 appear to induce similar increases in TNFα and sTNF-RII in patients, but only treatment with rIL2 results in VLS. These observations suggest that changes in cytokine levels alone are insufficient to induce vascular leakage and that other factors must be involved. Another difference between treatment groups in the current study was that it was difficult to draw blood samples and inject into the tail vein (veins easily collapsed) in rIL2-treated mice as compared with PBS and mIL21-treated mice (data not shown), perhaps due to hypotension in the rIL2-treated mice. Clinically, hypotension has been reported as a critical aspect of rIL2-induced toxicity.[1] In contrast, hypotension has been reported only infrequently in patients treated with rIL21 in multiple clinical trials[29,32,33] and was less severe than the hypotension reported for rIL2 therapy.[9,11,36] We did not measure blood pressure in our mice, and future studies incorporating blood pressure measurement need to be conducted to characterize hypotension in rIL2- and mIL21-treated mice.

Our histopathology findings were consistent with the gross and clinical pathology changes associated with the cytokine treatments. The rIL2-treated mice displayed dose-related increases in the incidence and severity of inflammatory cell infiltration in lung and liver. In comparison, inflammatory cell infiltrates were much less severe in mIL21-treated animals. The finding of inflammatory cell infiltrates in various tissues after administration of rIL2 is consistent with previous descriptions of the effects of rIL2 in mice.[17] These infiltrates have been characterized immunohistochemically as including cytotoxic T lymphocytes, NK cells, and lymphokine-activated killer cells.[18]

The current studies show that mIL21 does not induce an acute inflammatory response leading to extensive endothelial damage, fluid extravasation, and VLS in mice. In clinical studies, rIL21 at any dose level (0.3 to 50 µg/kg per dose) did not induce VLS in patients with cancer, and clinical benefit was demonstrated.[7,9,14] These preclinical and clinical data support the use of rIL21 as a less toxic alternative to rIL2 in cancer therapy.

References

1. **Acquavella N, Kluger H, Rhee J, Farber L, Tara H, Ariyan S, Narayan D, Kelly W, Sznol M.** 2008. Toxicity and activity of a twice0-daily high-dose bolus interleukin 2 regimen in patients with metastatic melanoma and metastatic renal cell cancer. J Immunother **31:**569–576.
2. **Anderson JA, Lentsch AB, Hadjiminas DJ, Miller FN, Martin AW, Nakagawa K, Edwards MJ.** 1996. The role of cytokines, adhesion molecules, and chemokines in interleukin-2–induced lymphocytic infiltration in C57BL/6 mice. J Clin Invest **97:**1952–1959.
3. **Anderson TD, Hayes TJ, Gately MK, Bontempo JM, Stern LL, Truitt GA.** 1988. Toxicity of human recombinant interleukin 2 in the mouse is mediated by interleukin-activated lymphocytes. Separation of efficacy and toxicity by selective lymphocyte subset depletion. Lab Invest **59:**598–612.
4. **Asao H, Okuyama C, Kumaki S, Ishii N, Tsuchiya S, Foster K, Sugamura K.** 2001. Cutting edge: the common γ-chain is an indispensable subunit of the IL21 receptor complex. J Immunol **167:**1–5.
5. **Baluna R, Vitetta ES.** 1997. Vascular leak syndrome: a side effect of immunotherapy. Immunopharmacology **37:**117–132.
6. **Becker TC, Noel RJ, Coats WS, Gomez-Foix AM, Alam T, Gerard RD, Newgard CB.** 1994. Use of recombinant adenovirus for metabolic engineering of mammalian cells. Methods Cell Biol **43 Pt A:**161–189.
7. **Brady J, Hayakawa Y, Smyth MJ, Nutt SL.** 2004. IL21 induces the functional maturation of murine NK cells. J Immunol **172:**2048–2058.
8. **Coquet JM, Kyparissoudis K, Pellicci DG, Besra G, Berzins SP, Smyth MJ, Godfrey DI.** 2007. IL21 is produced by NKT cells and modulates NKT cell activation and cytokine production. J Immunol **178:**2827–2834.
9. **Davis ID, Brady B, Kefford RF, Millward M, Cebon J, Skrumsager BK, Mouritzen U, Hansen LT, Skak K, Lundsgaard D, Frederiksen KS, Kristjansen PE, McArthur G.** 2009. Clinical and biological efficacy of recombinant human interleukin 21 in patients with stage IV malignant melanoma without prior treatment: a phase IIa trial. Clin Cancer Res **15:**2123–2129.
10. **Davis ID, Skak K, Smyth MJ, Kristjansen PE, Miller DM, Sivakumar PV.** 2007. Interleukin-21 signaling: functions in cancer and autoimmunity. Clin Cancer Res **13:**6926–6932.
11. **Davis ID, Skrumsager BK, Cebon J, Nicholaou T, Barlow JW, Moller NP, Skak K, Lundsgaard D, Frederiksen KS, Thygesen P, McArthur GA.** 2007. An open-label, 2-arm, phase I trial of recombinant human interleukin 21 in patients with metastatic melanoma. Clin Cancer Res **13:**3630–3636.
12. **Dodds MG, Frederiksen KS, Skak K, Hansen LT, Lundsgaard D, Thompson JA, Hughes SD.** 2009. Immune activation in advanced cancer patients treated with recombinant IL21: multianalyte profiling of serum proteins. Cancer Immunol Immunother **58:**843–854.
13. **Dubinett SM, Huang M, Lichtenstein A, McBride WH, Wang J, Markovitz G, Kelley D, Grody WW, Mintz LE, Dhanani S.** 1994. Tumor necrosis factor α plays a central role in interleukin-2–induced pulmonary vascular leak and lymphocyte accumulation. Cell Immunol **157:**170–180.
14. **Eriksen KW, Sondergaard H, Woetmann A, Krejsgaard T, Skak K, Geisler C, Wasik MA, Odum N.** 2009. The combination of IL21 and IFNα boosts STAT3 activation, cytotoxicity, and experimental tumor therapy. Mol Immunol **46:**812–820.
15. **Ettinger R, Sims GP, Fairhurst AM, Robbins R, da Silva YS, Spolski R, Leonard WJ, Lipsky PE.** 2005. IL21 induces differentiation of human naive and memory B cells into antibody-secreting plasma cells. J Immunol **175:**7867–7879.
16. **Fujita S, Puri RK, Yu ZX, Travis WD, Ferrans VJ.** 1991. An ultrastructural study of in vivo interactions between lymphocytes and endothelial cells in the pathogenesis of the vascular leak syndrome induced by interleukin 2. Cancer **68:**2169–2174.
17. **Gately MK, Anderson TD, Hayes TJ.** 1988. Role of asialo-GM1–positive lymphoid cells in mediating the toxic effects of recombinant IL2 in mice. J Immunol **141:**189–200.
18. **Harada Y, Yahara I.** 1998. Pathogenesis of toxicity with human-derived interleukin 2 in experimental animals. Int Rev Exp Pathol **34:**37–55.
19. **Institute for Laboratory Animal Research.** 1996. Guide for the care and use of laboratory animals. Washington (DC): National Academies Press.
20. **Kasaian MT, Whitters MJ, Carter LL, Lowe LD, Jussif JM, Deng B, Johnson KA, Witek JS, Senices M, Konz RF, Wurster AL, Donaldson DD, Collins M, Young DA, Grusby MJ.** 2002. IL21 limits NK-cell responses and promotes antigen-specific T-cell activation: a mediator of the transition from innate to adaptive immunity. Immunity **16:**559–569.
21. **Lentsch AB, Miller FN, Edwards MJ.** 1999. Mechanisms of leukocyte-mediated tissue injury induced by interleukin 2. Cancer Immunol Immunother **47:**243–248.

22. **Margolin K.** 2008. Cytokine therapy in cancer. Expert Opin Biol Ther **8:**1495–1505.
23. **McDermott DF, Atkins MB.** 2008. Immunotherapy of metastatic renal cell carcinoma. Cancer J **14:**320–324.
24. **Moroz A, Eppolito C, Li Q, Tao J, Clegg CH, Shrikant PA.** 2004. IL21 enhances and sustains $CD8^+$ T cell responses to achieve durable tumor immunity: comparative evaluation of IL2, IL15, and IL21. J Immunol **173:**900–909.
25. **Ozaki K, Spolski R, Ettinger R, Kim HP, Wang G, Qi CF, Hwu P, Shaffer DJ, Akilesh S, Roopenian DC, Morse HC 3rd, Lipsky PE, Leonard WJ.** 2004. Regulation of B-cell differentiation and plasma-cell generation by IL21, a novel inducer of Blimp 1 and Bcl 6. J Immunol **173:**5361–5371.
26. **Parrish-Novak J, Dillon SR, Nelson A, Hammond A, Sprecher C, Gross JA, Johnston J, Madden K, Xu W, West J, Schrader S, Burkhead S, Heipel M, Brandt C, Kuijper JL, Kramer J, Conklin D, Presnell SR, Berry J, Shiota F, Bort S, Hambly K, Mudri S, Clegg C, Moore M, Grant FJ, Lofton-Day C, Gilbert T, Rayond F, Ching A, Yao L, Smith D, Webster P, Whitmore T, Mauer M, Kaushansky K, Holly RD, Foster D.** 2000. Interleukin 21 and its receptor are involved in NK-cell expansion and regulation of lymphocyte function. Nature **408:**57–63.
27. **Peace DJ, Cheever MA.** 1989. Toxicity and therapeutic efficacy of high-dose interleukin 2. In vivo infusion of antibody to NK1.1 attenuates toxicity without compromising efficacy against murine leukemia. J Exp Med **169:**161–173.
28. **Pelletier M, Bouchard A, Girard D.** 2004. In vivo and in vitro roles of IL21 in inflammation. J Immunol **173:**7521–7530.
29. **Petrella T, Quirt I, Verma S, Haynes AE, Charette M, Bak K.** 2007. Single-agent interleukin 2 in the treatment of metastatic melanoma. Curr Oncol **14:**21–26.
30. **Rafi-Janajreh AQ, Chen D, Schmits R, Mak TW, Grayson RL, Sponenberg DP, Nagarkatti M, Nagarkatti PS.** 1999. Evidence for the involvement of CD44 in endothelial cell injury and induction of vascular leak syndrome by IL2. J Immunol **163:**1619–1627.
31. **Romo de Vivar Chavez A, de Vera ME, Liang X, Lotze MT.** 2009. The biology of interleukin-2 efficacy in the treatment of patients with renal cell carcinoma. Med Oncol **26 Suppl 1:**3–12.
32. **Rosenstein M, Ettinghausen SE, Rosenberg SA.** 1986. Extravasation of intravascular fluid mediated by the systemic administration of recombinant interleukin 2. J Immunol **137:**1735–1742.
33. **Schwartz RN, Stover L, Dutcher J.** 2002. Managing toxicities of high-dose interleukin 2. Oncology (Williston Park) **16:**11–20.
34. **Sondergaard H, Frederiksen KK, Thygesen P, Galsgaard ED, Skak K, Kristijansen PE, Odum N, Kragh M.** 2007. Interleukin-21 therapy increases the density of tumor infiltrating $CD8^+$ T cells and inhibits the growth of syngeneic tumors. Cancer Immunol Immunother **56:**1417–1428.
35. **Spolski R, Leonard WJ.** 2008. Interleukin 21: basic biology and implications for cancer and autoimmunity. Annu Rev Immunol **26:**57–79.
36. **Thompson JA, Curti BD, Redman BG, Bhatia S, Weber JS, Agarwala SS, Sievers EL, Hughes SD, DeVries TA, Hausman DF.** 2008. Phase I study of recombinant interleukin 21 in patients with metastatic melanoma and renal cell carcinoma. J Clin Oncol **26:**2034–2039.
37. **Vial T, Descotes J.** 1992. Clinical toxicity of interleukin 2. Drug Saf **7:**417–433.
38. **Waggie KS, Holdren MS, Byrnes-Blake K, Pedersen S, Ponce R, Hughes S, Miller DM.** 2012. Preclinical safety, pharmacokinetics, and pharmacodynamics of recombinant IL21 in cynomolgus (*Macaca fascicularis*) macaques. Int J Toxicol **31:**303–316.